Diallyl disulfide induces G2/M arrest and promotes apoptosis through the p53/p21 and MEK-ERK pathways in human esophageal squamous cell carcinoma

XIAORAN YIN[1], RONG ZHANG[4], CHENG FENG[2], JUN ZHANG[2], DONG LIU[2], KUN XU[1], XIJING WANG[1], SHUQUN ZHANG[1], ZONGFANG LI[3], XINLIAN LIU[1] and HONGBING MA[1]

Departments of [1]Oncology, [2]Digestion and [3]General Surgery, The Second Affiliated Hospital of Xi'an Jiaotong University, Xi'an, Shaanxi 710004; [4]Department of Gastroenterology, Shaanxi Provincial People's Hospital, Xi'an, Shaanxi 710068, P.R. China

Received May 8, 2014; Accepted July 8, 2014

DOI: 10.3892/or.2014.3361

Abstract. Esophageal squamous cell carcinoma (ESCC) is an aggressive tumor with high incidence and mortality worldwide. Diallyl disulfide (DADS) is a natural organosulfur compound, isolated from garlic. In this study, MTT assay showed that DADS significantly reduced cell viability in a dose- and time-dependent manner in ESCC cells, with lower toxicity in normal liver cells. Cell cycle analysis revealed that DADS made G2/M phase arrest. Molecular analysis suggested that this cell cycle arrest was likely made by the decrease of cyclin B1, cdc2, p-cdc2, cdc25c in concomitance with activation of the p53/p21 pathway. Apoptosis was detected by Annexin V/PI staining. The molecule markers showed that DADS induced apoptosis through activating caspases, altering the Bax/Bcl-2 balance and suppressing the MEK-ERK pathway. Our data indicated that DADS has the potential to be an effective and safe anticancer agent for ESCC therapy in the near future.

Introduction

Esophageal squamous cell carcinoma (ESCC) is one of the most refractory malignant diseases worldwide, and more than 50% of cases occur in China. Increasing rates of morbidity and mortality of ESCC have been reported in recent years (1). Current treatment generally employs surgical resection combined with chemotherapy and radiotherapy for advanced ESCC. However, both the high recurrence rate and strong systemic toxicity of the anticancer treatments led us to investigate new agents to improve the therapeutic effect (2).

In recent years, plant food-derived phytochemical anticancer strategies have been proposed to control various types of carcinoma (3). Diallyl disulfide (DADS), CH2=CH-CH2-S-S-CH2CH=CH2, is one of the fat-soluble sulfur compounds obtained from crushed garlic and represents 40-60% of garlic essential oil (4). DADS has a wide variety of biological activities including antifungal (5), antibacterial (6), antiviral (7), antioxidant (8), antiplatelet and antithrombotic properties (9). Moreover, DADS has gained increasing attention due to its protective effects of cancer development and anticancer effects against different types of malignancies (10-13). Notably, the apoptotic effects of DADS were even superior to those of chemotherapy agents such as 5-Fu and CTX in human breast cancer cells (14).

Apoptosis is an ordered and orchestrated cellular process that occurs in physiological and pathological conditions, which plays an important role in the treatment of cancer (15-17). The exact mechanism of DADS on ESCC is still unclear. The ability of DADS to control tumor growth may be due to its capacity to interfere different pathways presented in the cell.

In the present study, we characterized the effects of DADS on ESCC cell line ECA109. Our results support the use of DADS as a potent anticancer drug by disrupting cell viability, arresting G2/M cell cycle arrest and inducing apoptosis of ECA109 cells. These data suggest that DADS may be a suitable candidate for the treatment of ESCC in the future.

Materials and methods

Materials. ECA109 human ESCC cell line and L02 human normal liver cell line were purchased from the Chinese Academy of Shanghai Institute of Cell Biology. DADS, dimethyl sulfoxide (DMSO), 3-(4,5-dimethylthiazol-2-yl)-2,5-diphenyl-tetrazolium bromide (MTT), bovine serum albumin (BSA), propidium iodide (PI), RNase A and phosphate-buffered saline (PBS) were purchased from Sigma Aldrich (USA). Fetal bovine serum (FBS), RPMI-1640 medium and 0.25% trypsin digest were purchased from Hyclone Co. (USA). TRIzol reagent was purchased from Invitrogen (USA). Annexin V conjugated to FITC (Annexin V-FITC) apoptosis kit was purchased from Roche Technology Co. (USA). PrimeScript™ RT Master Mix kit, SYBR® Premix Ex Taq II were purchased from Takara

Correspondence to: Professor Hongbing Ma, Department of Oncology, The Second Hospital of Xi'an Jiaotong University, 157 Xiwu Road, Xi'an, Shaanxi 710004, P.R. China
E-mail: mhbxian@126.com

Key words: diallyl disulfide, apoptosis, G2/M, p53/p21, MEK-ERK

Table I. Primers for real-time PCR analysis.

Gene	Forward sequence	Reverse sequence
β-actin	5'-TGGCACCCAGCACAATGAA-3'	5'-CTAAGTCATAGTCCGCCTAGAAGCA-3'
p21	5'-AACATGTTGAGCTCTGGCATAGAAG-3'	5'-GCATGGGTTCTGACGGACA-3'
p53	5'-TCAGCATCTTATCCGAGTGGAA-3'	5'-TGTAGTGGATGGTGGTACAGTCA-3'
Bcl-2	5'-GTGTGGAGAGCGTCAACC-3'	5'-CTTCAGAGACAGCCAGGAG-3'
Bax	5'-ATGGGCTGGACATTGGACTTC-3'	5'-TGGTGAGTGAGGCGGTGAG-3'

Technology Company (Japan). Enhanced chemiluminescence (ECL) kit was purchased from Amersham Life Sciences (UK). Antibodies to ERK1/2, phospho-ERK1/2 (p-ERK1/2), MEK1, phospho-MEK1 (p-MEK1), and caspase-3, cleaved caspase-3, cyclin B1, cdc2, phospho-cdc2 (p-cdc2), cdc25c, and PCNA were purchased from Cell Signaling Technology Co. (USA). β-actin antibody was purchased from Santa Cruz Biotechnology (USA). Horseradish peroxidase (HRP)-coupled goat anti-mouse IgG and anti-rabbit IgG (secondary antibody) were purchased from Santa Cruz Biotechnology (USA).

Cell culture. Human ECA109 cell line and human L02 cell line were cultured in RPMI-1640 supplemented with 10% FBS, 100 U/ml penicillin G and 100 μg/ml streptomycin sulfate, at 37˚C with 5% CO_2. The medium was replaced every other day. After reaching 70-80% confluency, cells were digested with 0.25% trypsin and subcultured. Exponentially growing cells were used for assays.

Cell viability assay. Cell viability was determined by using MTT assay. DADS was dissolved in PBS with less than 0.01% DMSO and prepared at a concentration of 1,000 μg/ml. PBS with less than 0.01% DMSO was used as the negative control. ECA109 and L02 cells were seeded in 96-well plates at $1x10^4$ cells/well and incubated with DADS (10-60 μg/ml). After incubation, 20 μl MTT (5 mg/ml) was added to each well. Four hours later, the blue crystals were solubilized with 150 μl DMSO. The absorbance was measured at 570 nm. The following formula was used for the calculation: Cell viability ratio = 1 - [(A value of the control - A value of the experimental samples)/A value of the control] x 100%. Half maximal inhibitory concentration (IC_{50}) values were calculated by SPSS® software. Each assay was performed in 5 replicates.

Cell cycle assay. A total of $5x10^5$ ECA109 cells/plate in 6 cm plates were incubated with different concentrations of DADS (20, 40, 60 μg/ml). PBS with less than 0.01% DMSO was used as control. Following 24 h treatment, cells were fixed with ice-cold 70% ethanol overnight at -20˚C, then stained with 5 μl PI at room temperature for 30 min in the dark. Finally, cell cycle analysis was performed using Flow Cytometer, and data were analyzed with Cell Quest Pro® software. The experiments were repeated three times.

Apoptosis assay. The apoptotic ratios of cells were determined with the Annexin V-FITC apoptosis detection kit. A total of $5x10^5$ ECA109 cells/plate in 6 cm plates were incubated with different concentrations of DADS (20, 40, 60 μg/ml). Cells treated with PBS with less than 0.01% DMSO were used as control. The cells were trypsinized, washed twice with PBS, resuspended in 100 μl of binding buffer at a concentration of $1x10^6$ cells/ml, incubated with 5 μl Annexin V-FITC and 10 μl PI for 15 min at room temperature in the dark, and added with 400 μl binding buffer. Apoptosis analysis was performed by Flow Cytometer, and data were analyzed with Cell Quest Pro software. The experiments were repeated at least three times.

Real-time polymerase chain reaction (PCR). Cells were treated with serially diluted concentrations of DADS (20, 40, 60 μg/ml) and harvested for 24 h. PBS with less than 0.01% DMSO was used as control. Total RNA was extracted by the TRIzol method and the quantity of RNA was assessed by spectrophotometry. cDNA was obtained by reverse transcription with 1 μg total RNA using PrimeScript™ RT Master Mix kit. Real-time PCR was performed with the SYBR-Premix Ex Taq™ II Perfect Real Time kit. All reactions were performed on an ABI QPCR System. The individual values were normalized to the β-actin control, and the ratio of the relative expression levels was calculated. The specific primers are shown in Table I. The samples were run in triplicate.

Western blot assay. ECA109 cells were prepared by serially diluted concentrations of DADS (20, 40, 60 μg/ml). Cells treated with PBS with less than 0.01% DMSO were used as control. After incubation for 24 h, cells were harvested to obtain protein concentrations by RIPA lysis buffer. Proteins (50 μg) were separated by 8-12% sodium dodecyl sulfate-polyacrylamide gel electrophoresis (SDS-PAGE), transferred to polyvinylidene difluoride (PVDF) membranes, then probed with appropriate primary antibodies. HRP-conjugated goat anti-mouse antibody or anti-rabbit antibody (1:10,000) was used as the secondary antibody. Antigen-antibody complex signals were visualized with BeyoECL Plus. The densitometric analysis was performed by Image J® software. The experiments were repeated three times.

The following primary antibodies were used: anti-cyclin B1 (1:1,000), anti-cdc2 (1:1,000), anti-p-cdc2 (1:500), anti-cdc25c (1:1,000), anti-ERK1/2 (1:1,000), anti-p-ERK1/2 (1:300), anti-caspase-3 (1:1,000), anti-cleaved caspase-3 (1:500), anti-MEK1 (1:1,000), anti-p-MEK1 (1:500) and anti-β-actin (1:1,000) antibodies.

Quantification and statistical analysis. Quantitative data are expressed as the mean ± SD from at least three independent

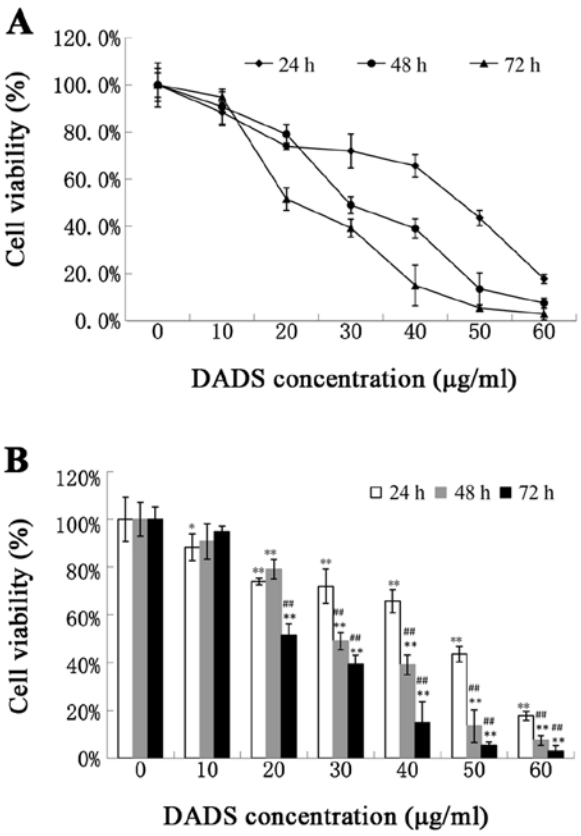

Figure 1. Viability inhibition effects of DADS on ECA109 cells by MTT assay. (A) ECA109 cells were incubated with different concentrations of DADS for 24, 48 and 72 h. (B) Cell viability was detected by MTT assay. Data are expressed as the mean ± SD from three independent experiments. *P<0.05, **P<0.01 vs. control group, ##P<0.01 vs. 24-h group.

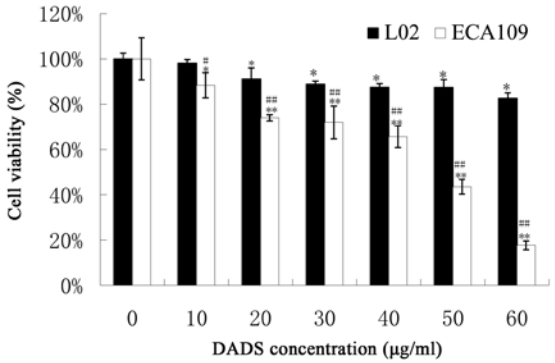

Figure 2. Viability inhibition effects of DADS on ECA109 and L02 cells by MTT assay. ECA109 and L02 cells were incubated with different concentrations of DADS for 24 h. Cell viability was detected by MTT assay. Data are expressed as the mean ± SD from three independent experiments. *P<0.05, **P<0.01 vs. control group, #P<0.05 and ##P<0.01 ECA109 group vs. L02 group.

Table II. Effect of DADS on the cell cycle of ECA109 cells.

Groups	N	G0/G1	G2/M	S
Control	3	60.01±3.13	13.43±1.25	26.56±2.02
20 μg/ml	3	48.51±2.65[a]	28.43±2.56[a]	23.06±2.45[b]
40 μg/ml	3	42.08±1.12[a]	39.90±2.06[a]	18.02±1.24[b]
60 μg/ml	3	18.97±1.37[a]	58.65±3.79[a]	22.38±2.56[b]

Data are expressed as the mean ± SD from three independent experiments. [a]P<0.01, [b]P<0.05 vs. control group.

experiments. The two-tailed Student's t-test was performed for paired samples, one-way analysis of variance (ANOVA) or two-factor factorial ANOVA was used for multiple groups. Results were considered to indicate a statistically significant difference at the P<0.05 level. Statistical analyses were performed by SPSS 17.0 statistical software.

Results

DADS inhibits cell viability. The MTT assay was used to detect the viability effects of DADS at various concentrations (10-60 μg/ml) on ECA109 and L02 cells. Our data showed that DADS clearly inhibited cell viability at the concentrations of 10-60 μg/ml following exposure for 24 h (P<0.05, Fig. 1), 20-60 μg/ml for 48 and 72 h (P<0.01, Fig. 1) compared with the control group. The IC_{50} was 49.02±4.78, 33.14±5.02 and 22.74±4.05 μg/ml for 24, 48 and 72 h DADS treatment respectively. The 72-h treatment group had an apparent difference compared with the 24-h treatment group (P<0.05, Fig. 1). DADS had less of an influence on L02 normal cells than on ECA109 esophageal carcinoma cells (P<0.05, Fig. 2). These results indicate that DADS significantly inhibited ECA109 cell viability in a dose- and time-dependent manner, and had a lower effect on normal cells.

DADS induces G2/M phase cell cycle arrest. Cell cycle distribution of ECA109 cells treated with different doses of DADS for 24 h was analyzed by flow cytometry. Results showed that the percentage of cells in the DADS groups, particularly at the 20, 40, 60 μg/ml concentrations, significantly increased at the G2/M phase in a dose-dependent manner compared with the control group. The percentage of cells at the G2/M phase increased from 13.43±1.25 to 58.65±3.79%, and decreased from 60.01±3.13 to 18.97±1.37% and from 26.56±2.02 to 22.38±2.56%, at the G0/G1 and S phase, respectively (Table II). These results suggest that DADS induced cell cycle arrest at the G2/M phase (Fig. 3), which may be one of the reasons for the viability inhibition and apoptosis induction of ECA109 cells.

DADS induces cell apoptosis. ECA109 cells were examined by phase contrast microscopy after incubation with DADS at different concentrations (20, 40, 60 μg/ml) for 24 h. Cells treated with PBS were used as control. The control group cells showed a typical polygonal and intact appearance, whereas the DADS-treated cells displayed dose-dependent changes in cell shape, such as membrane blebbing, formation of apoptotic bodies, cellular shrinkage, poor adherence and floating shapes (Fig. 4).

The suppression of cancer cell growth correlates with apoptosis. We explored the apoptosis rate of ECA109 cells impacted with different concentrations of DADS for 24 h with Annexin V-FITC and PI staining observed by flow cytometry. The rate of apoptosis in the control and DADS groups (20, 40

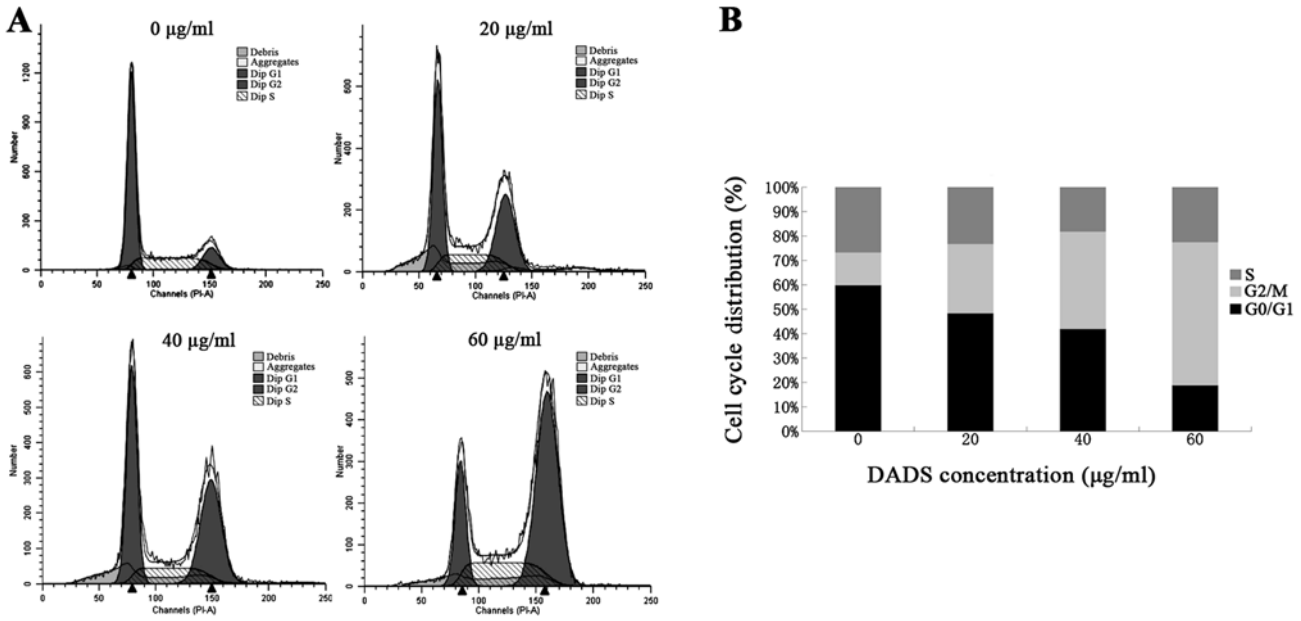

Figure 3. Effects of DADS on the G2/M phase arrest of ECA109 cells by flow cytometry. ECA109 cells were treated with different concentrations of DADS for 24 h. (A) Cell cycle proportions were determined by flow cytometry. (B) The percentage of cells in G0/G1, S, and G2/M phase. Data are expressed as the mean ± SD from three independent experiments.

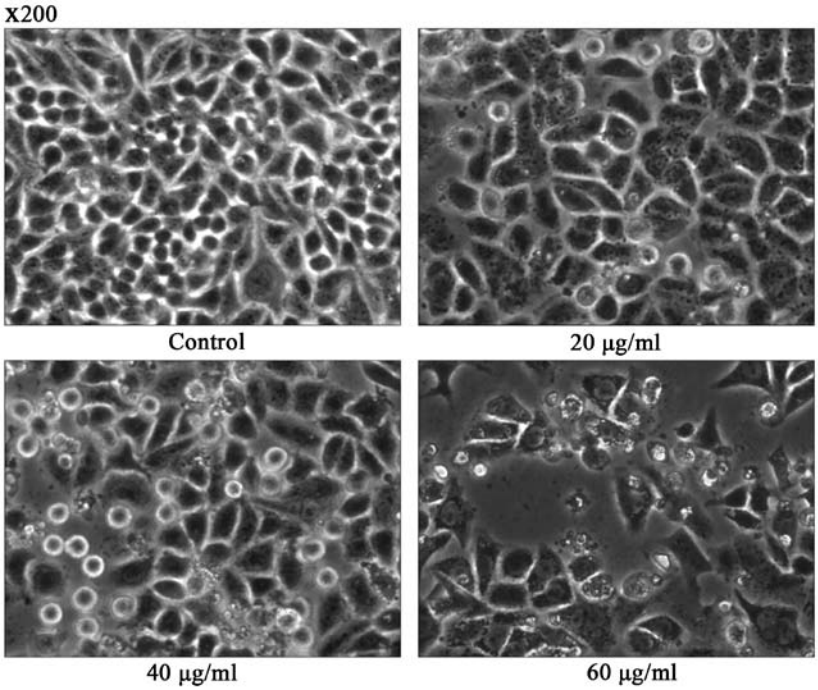

Figure 4. Morphology of ECA109 cells treated with DADS. Morphology of cells treated with different concentrations of DADS for 24 h under phase contrast microscopy (magnification, x200).

and 60 μg/ml) for 24 h was 10.26±1.05, 14.48±0.99, 42.68±2.08 and 72.96±3.43% respectively (P<0.05, Fig. 5). These results demonstrate that DADS induced apoptosis of ECA109 cells in a dose-dependent manner.

DADS inhibits G2/M phase-associated protein expression of cyclin B1, cdc2, p-cdc2 and cdc25c. Since DADS induced G2/M phase arrest in ECA109 cells, we evaluated the expression of proteins that regulate the G2/M phase transition by western blot assay. Cyclin B1, cdc2, and cdc25c are important proteins related to the G2/M phase. G2/M phase is controlled by a complex formed cyclin B1 and cdc2, and the complex is regulated by cdc25c. Our data showed that cdc2 protein levels had no apparent change (P>0.05, Fig. 6), and the protein levels of cyclin B1 and cdc25c decreased in a dose-dependent manner with significant inhibition occurring at DADS concentrations of 40 and 60 μg/ml (P<0.01, Fig. 6). Moreover, the protein levels of p-cdc2 decreased in a dose-dependent manner, with

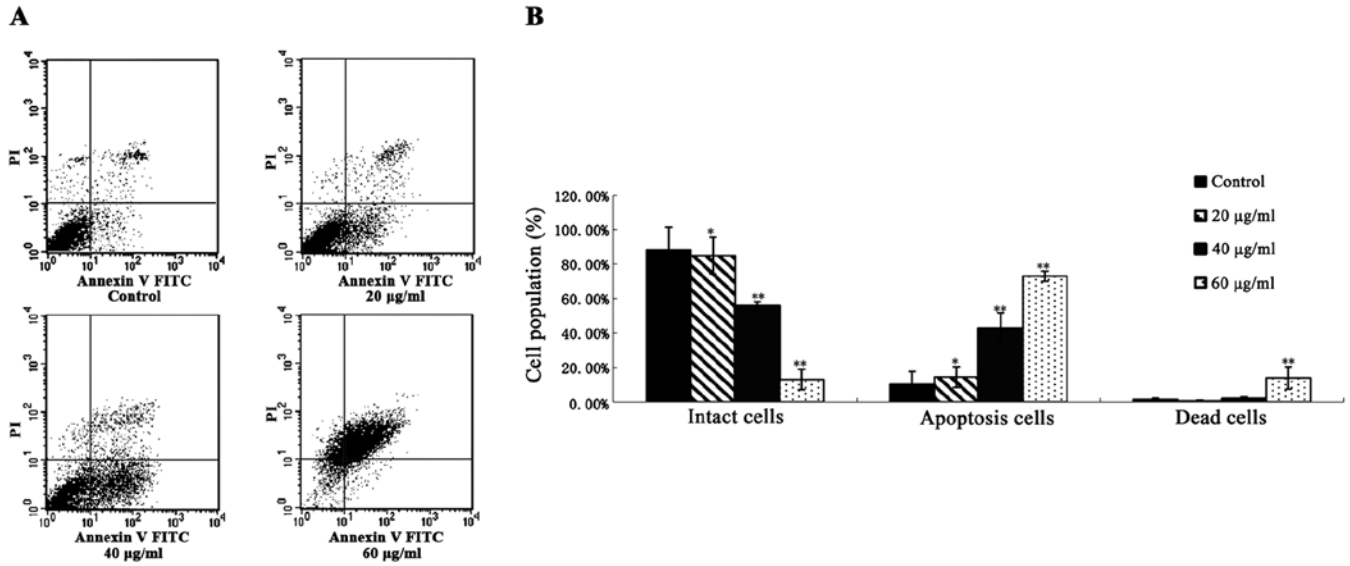

Figure 5. Effects of DADS on the apoptosis induction of ECA109 cells by flow cytometry. ECA109 cells were treated with different concentrations of DADS for 24 h. (A) Apoptosis was assessed by Annexin V-PI double staining. (B) Statistical analysis of apoptosis rate. Data are expressed as the mean ± SD from three independent experiments. *P<0.05, **P<0.01 vs. control group.

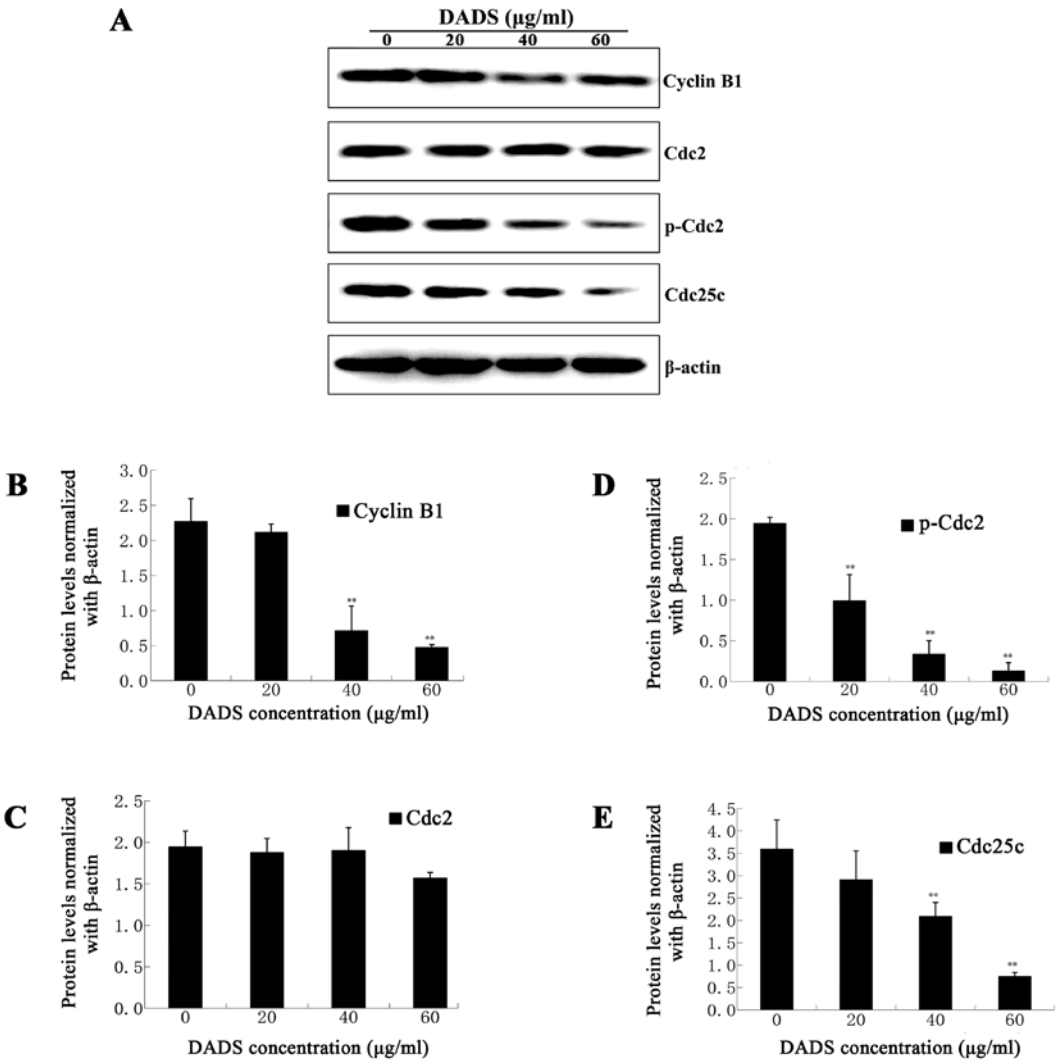

Figure 6. Expression levels of cyclin B1, cdc2, p-cdc2 and cdc25c detected by western blotting in ECA109 cells treated with DADS. Cells were treated with different concentrations of DADS for 24 h. The expression of proteins was assessed by western blotting. Representative blots (A), and densitometric analysis of DADS on the expression of cyclin B1 (B), cdc2 (C), p-cdc2 (D) and cdc25c (E) are shown. Data are expressed as the mean ± SD from three independent experiments. **P<0.01 vs. control group.

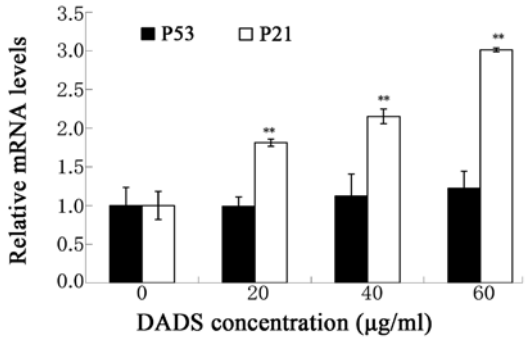

Figure 7. Effects of DADS on the levels of p53 and p21 mRNA expression by real-time PCR assay in ECA109 cells. Cells were treated with different concentrations of DADS for 24 h. The expression levels of p53 and p21 mRNAs were assessed by real-time PCR assay. Data are expressed as the mean ± SD from three independent experiments. **P<0.01 vs. control group.

significant inhibition occurring at DADS concentrations of 20, 40 and 60 μg/ml (P<0.01, Fig. 6). These results indicate that DADS reduced the expression of cyclin B1, p-cdc2, and cdc25c to induce G2/M phase arrest of ECA109 cells.

Effects of DADS on the p53/p21 pathway. The p53/p21 pathway is involved in the cell apoptosis progression and plays an important role in the cell cycle arrest of G2/M phase. Therefore, we used real-time PCR assay to investigate the G2/M phase relative molecular pathway. Our data showed that DADS (20, 40 and 60 μg/ml) upregulated mRNA levels of p21 (P<0.01, Fig. 7), p53 (P<0.05, Fig. 7) compared with the relative control. The upregulated levels of p21 mRNA expression were accompanied by the increase of G2/M arrest. Based on these results, we suggest that DADS-increased G2/M phase arrest and apoptosis rate of ECA109 cells might be partly affected by the p53/p21 signaling pathway.

Protein expression of caspase-3 and cleaved caspase-3 by western blot analysis. As the imbalance of apoptotic signals is closely related to the initiation of the apoptotic program, we analyzed the protein expression levels of caspase-3 and cleaved caspase-3 proteins by western blotting. These proteins were blotted against the corresponding antibodies as mentioned above in the ECA109 cells, following 24 h of treatment with DADS (20, 40 and 60 μg/ml). Our results showed that the protein levels of caspase-3 increased at DADS doses of 40 and 60 μg/ml (P<0.01, Fig. 8), and the expression levels of cleaved caspase-3 fragment (17 kDa, 19 kDa) were clearly upregulated in a dose-dependent manner, particularly at 20, 40 and 60 μg/ml doses (P<0.01, Fig. 8). Therefore, this study suggests that DADS-induced apoptosis of ECA109 cells is mediated by effector caspase-3.

Effects of DADS on Bax, Bcl-2 expression levels and Bax/Bcl-2 ratio. DADS-induced apoptosis of ECA109 cells prompted an examination of certain apoptosis regulatory proteins, such as Bax and Bcl-2. The expression levels of Bax mRNA significantly increased in 40 and 60 μg/ml (P<0.05, Fig. 9), whereas the expression levels of Bcl-2 mRNA were clearly decreased in 20, 40 and 60 μg/ml (P<0.01, Fig. 9). The Bax/Bcl-2 ratio was significantly increased in the presence of DADS at concentrations of 40 and 60 μg/ml (P<0.05, Fig. 9). Collectively, the data

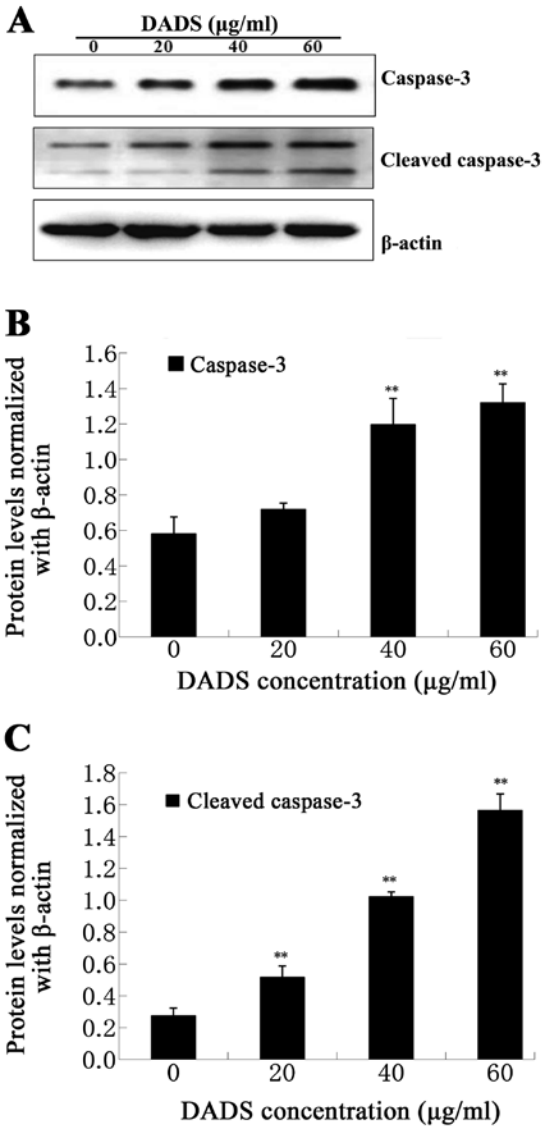

Figure 8. Expression levels of caspase-3 and cleaved caspase-3 detected by western blotting in ECA109 cells treated with DADS. ECA109 cells were treated with different concentrations of DADS for 24 h. Protein expression levels were determined by western blot analysis. Representative blots (A) and densitometric analysis of DADS on the expression of caspase-3 (B), cleaved caspase-3 (C) are shown. Data are expressed as the mean ± SD from three independent experiments. **P<0.01 vs. control group.

suggest that DADS induced apoptosis through upregulation of Bax mRNA, downregulation of Bcl-2 mRNA and a shift of Bax/Bcl-2 ratio in a dose-dependent manner.

Effects of DADS on the MEK-ERK pathway. Western blot analysis was used to evaluate the effect of DADS on MEK1, ERK1/2 and their phosphorylation levels in ECA109 cells. Our data showed that the protein levels of MEK1 and ERK1/2 had no obvious change, whereas the expression levels of p-MEK1 and p-ERK1/2 were clearly decreased in the 20, 40 and 60 μg/ml DADS groups compared with the control (P<0.01, Fig. 10). As shown in Fig. 10, DADS inhibited p-MEK1 and p-ERK1/2 in a dose-dependent manner. Based on these results, we suggest that DADS-related apoptosis in ECA109 cells might be influenced by the MEK-ERK signaling pathway.

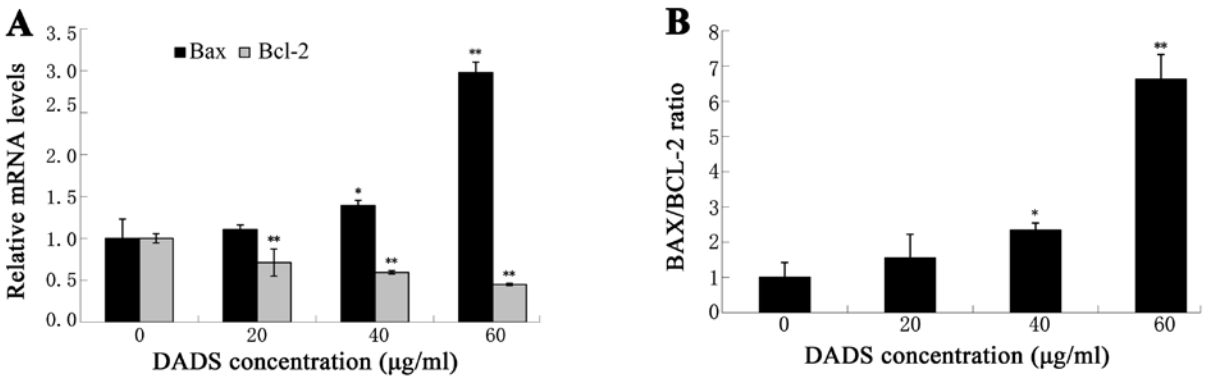

Figure 9. Effects of DADS on the levels of Bax and Bcl-2 mRNA expression by real-time PCR assay in ECA109 cells. The expression of Bax and Bcl-2 mRNA influenced by different concentrations of DADS in ECA109 cells were assessed by real-time PCR. (A) mRNA expression of Bax and Bcl-2. (B) Bax/Bcl-2 ratio. Data are expressed as the mean ± SD from three independent experiments. *P<0.05, **P<0.01 vs. control group.

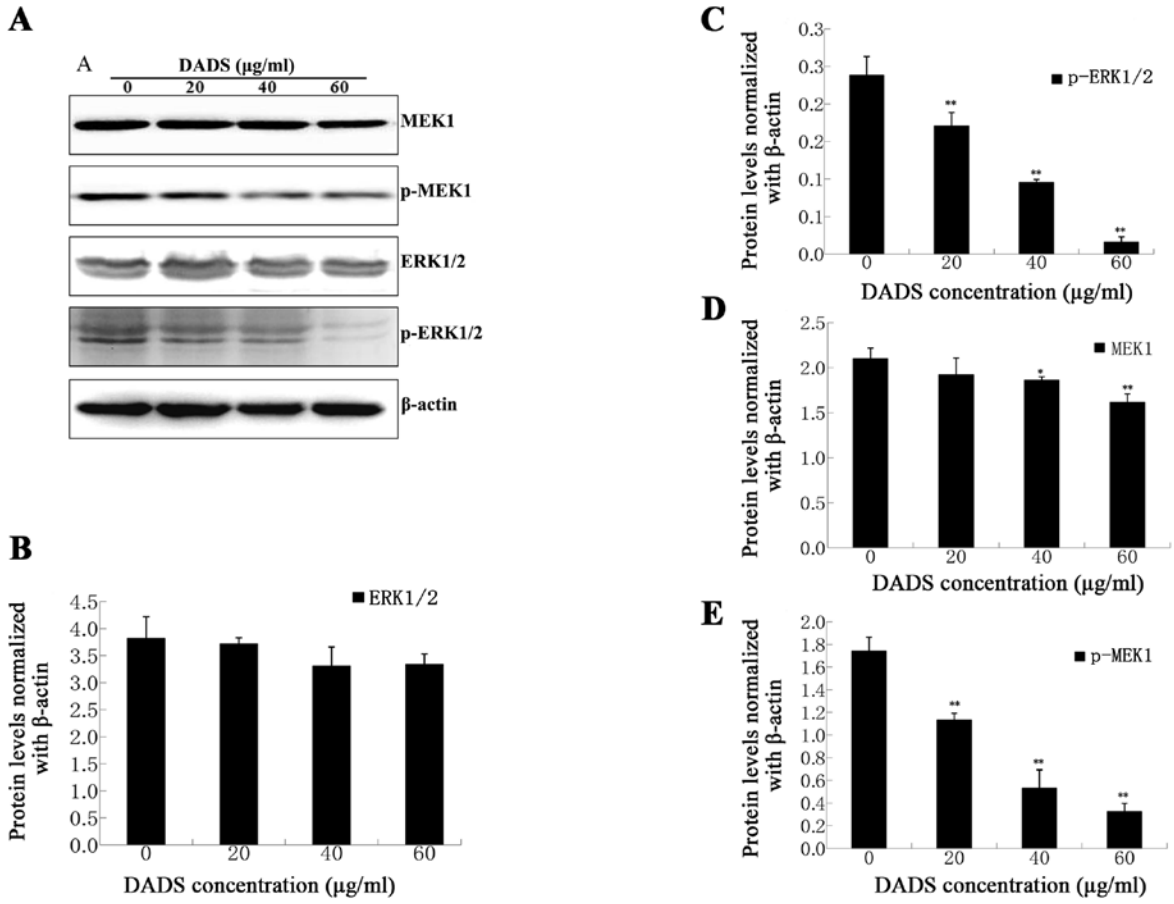

Figure 10. Effects of DADS on the MEK-ERK pathway assessed by western blotting in ECA109 cells. ECA109 cells were treated with different concentrations of DADS. Levels of MEK1, p-MEK1 and ERK1/2, p-ERK1/2 were assessed by western blot analysis. Representative blots (A) and densitometric analysis of DADS on the expression of MEK1 (B), p-MEK1 (C), ERK1/2 (D) and p-ERK1/2 (E) are shown. Data are expressed as the mean ± SD from three independent experiments. *P<0.05, **P<0.01 vs. control group.

Discussion

Diallyl disulfide (DADS) is a lipid-soluble organic compound from garlic. Scientific investigations have shown that DADS can reduce the risk of cardiovascular disease and diabetes, stimulate the immune system, protect against infections, and show significant protection against different types of malignancies (4,18).

By MTT assay, DADS showed dose- and time-dependent anti-viability effects on ESCC cell lines (Figs. 1 and 2). Moreover, we further demonstrated that DADS had much lower cytotoxicity in L02 normal liver cells compared with ECA109 carcinoma cells (P<0.01). The viability inhibitory properties of DADS may be attributable to its induction of cell cycle arrest and apoptosis cell death, which is consistent with previous findings (10-13).

G2/M phase cell cycle arrest can reduce proliferation and induce apoptosis by inhibiting the segregation of damaged chromosomes during mitosis (15). DADS has been demonstrated to induce G2/M cell cycle arrest in several cancer cell lines such as colon cancer (11), breast cancer (12) and human gastric cancer cells (13). In the present study, we demonstrated that the percentage of ECA109 cells in DADS treatment groups significantly increased at the G2/M phase in a dose-dependent manner (Fig. 3). The G2/M phase arrest induced by DADS showed an increase in the number of ECA109 cells from 13.43 to 58.65%, as well as apoptotic cells from 10.2 to 72.96% (Table II), suggesting that the block in the G2/M phase results in triggering the apoptotic program.

Apoptosis is a morphologically and biochemically distinct mode of cell death that plays major roles during carcinogenesis, cancer treatment and toxic cell killing (19). Apoptosis induction involves different apoptotic genes and enzymes depending on the cell type of different tumors (16). DADS has the ability to induce apoptosis of human tumor cells including those of colon, gastric, prostate and breast origin (10,11,18,20-22). Our study confirmed the apoptotic effects of DADS on ECA109 cells by using several methods. First, under light microscope, we observed that morphological changes of apoptosis were induced by DADS. Typical morphological characteristics of apoptotic ECA109 cells, such as membrane blebbing, cell shrinkage and formation of apoptotic bodies, were observed in the 40, 60 μg/ml DADS dose group (Fig. 4). Second, we detected the apoptosis rate by the double-staining of Annexin V-FITC and PI. Our flow cytometry analysis showed that DADS promoted ECA109 apoptosis in a dose-dependent manner (Fig. 5).

DADS controlled tumor growth and death. Although the mechanism for DADS-induced apoptosis has been studied in several cellular systems, it remains a controversial issue. As the balance and interplay of multiple signaling networks involved in various signaling contexts, it is not surprising that DADS regulation is complex. Therefore, the results of the present study indicate the noticeable changes in molecular signals of ECA109 cells affected by DADS.

G2/M phase progression is regulated by cdc2 kinases and cyclin B1. In addition, cdc2 activation depends on the dephosphorylation of Tyr15 by cdc25c. Otherwise, p53 and the p53-responsive gene, p21, can suppress cyclin B1 and cdc2 expression by inhibiting either cdc2 kinase activity or blocking the interaction of cyclin B1-cdc2 complexes with their substrates, leading to G2/M-phase cell cycle arrest (23-27). Furthermore, the MEK-ERK pathway has crosstalk with p53/p21, and Bax is a key target of the p53 transcription process in aspects of cell apoptosis (26). In the case of our study, the data showed that DADS downregulated cyclin B1, cdc2, p-cdc2 and cdc25c expression (Fig. 7) and upregulated p21 expression of ECA109 cells in a dose-dependent manner (Fig. 6). Thus, we found that upregulation of the p53/p21 pathway could be due to blocking the interaction of cyclin B1-cdc2 complexes, and downregulation of cdc25c consequently reduced the activity of cdc2. Therefore, we suggest that alterations in G2/M phase-associated protein levels and p53/p21 signaling pathway may be the mechanism underlying the growth inhibition and G2/M phase arrest.

Bax is a key target of the p53 transcription process in aspects of cell apoptosis (26). Anti-apoptotic protein Bcl-2 could bind to and inactivate Bax and other pro-apoptotic proteins to inhibit apoptosis. Therefore, Bax/Bcl-2 ratio plays a pivotal role in apoptosis (28). Moreover, caspase-3 plays an important role as the central effector for initiation of apoptosis (16). Our results suggest that DADS promoted cell death by downregulating Bcl-2 mRNA expression and upregulating the Bax expression in a dose-dependent manner, thus increasing the Bax/Bcl-2 ratio (Fig. 9), leading to a pro-apoptotic process via caspase-3 in ECA109 cells (Fig. 8). Based on these observations, the data indicate that the increase of Bax/Bcl-2 and activation of caspase-3 are involved in the DADS-induced apoptosis mechanism.

The sequential phosphorylation of MAPK kinase1/2 (MEK1/2) makes the activation of extracellular signal-regulated kinase1/2 (ERK1/2). Then, ERK1/2 activation leads to phosphorylation of a variety of transcription factors and results in proliferation and differentiation, protecting cells against apoptosis (29). MEK-ERK signaling cascade may be affected by the activation of the p53/p21 pathway (26). Although DADS was reported to rapidly and potently inhibit the phosphorylation of ERK1/2 to induce apoptosis in human leukemia cell line HL-60 (21), other studies showed that DADS activated ERK1/2 in human non-small cell lung carcinoma H1299 cell death (20). Our results showed that both p-MEK1 and p-ERK1/2 were inhibited following DADS treatment in a dose-dependent manner (Fig. 10), suggesting that the MEK-ERK pathway plays a role in maintaining the regulation of apoptosis by DADS in ECA109 cells.

In summary, the present study confirmed that DADS inhibits ESCC cell viability with only a slight effect on normal cells. To the best of our knowledge, this is the first report to identify mechanisms of the antitumor properties of DADS in human ESCC cells. DADS has been shown to arrest cancer cells at the G2/M phase via the modulation of cell-cycle related proteins, which is associated with the reduction of cyclin B1, cdc2, p-cdc2, cdc25c expression. Furthermore, DADS controlled cellular apoptosis by activating caspase-3, upregulating Bax/Bcl-2 ratio and downregulating the MEK-ERK signaling pathway. Moreover, activation of the p53/p21 pathway is involved in the process of inhibiting cell differentiation, arresting G2/M phase and inducing apoptosis. In brief, DADS regulates ESCC cells via multiple networks involved in various signaling contexts. Therefore, this study suggests that DADS may be a promising anticancer therapeutic for ESCC in the near future.

Acknowledgements

This study was supported by funds from the Science and Technology Program of Shaanxi Province (nos. 2010K01-141 and 2011K13-02-05), the Important Clinic Project of the Chinese Ministry of Health (no. 2007353). This study was also supported by the Office of Oncology Research (Zong-Fang Li). The authors are grateful to Dr Guleng B for his technical assistance.

References

1. Cui X, Zhao Z, Liu D, *et al*: Inactivation of miR-34a by aberrant CpG methylation in Kazakh patients with esophageal carcinoma. J Exp Clin Cancer Res 33: 20-33, 2014.

2. Orditura M, Galizia G, Fabozzi A, *et al*: Preoperative treatment of locally advanced esophageal carcinoma. Int J Oncol 43: 1745-1753, 2013.
3. Matés JM, Segura JA, Alonso FJ and Márquez J: Anticancer antioxidant regulatory functions of phytochemicals. Current Medicinal Chemistry. 18: 2315-2338, 2011.
4. Zhou Y, Su J, Shi L, Liao Q and Su Q: DADS downregulates the Rac1-ROCK1/PAK1-LIMK1-ADF/cofilin signaling pathway, inhibiting cell migration and invasion. Oncol Rep 29: 605-612, 2013.
5. Alam M, Zubair S, Farazuddin M, *et al*: Development, characterization and efficacy of niosomal diallyl disulfide in treatment of disseminated murine candidiasis. Nanomedicine 9: 247-256, 2013.
6. Maldonado PD, Chánez-Cárdenas ME and Pedraza-Chaverrí J: Aged garlic extract, garlic powder extract, S-allylcysteine, diallyl sulfide and diallyl disulfide do not interfere with the antibiotic activity of gentamicin. Phytother Res 19: 252-254, 2005.
7. Lissiman E, Bhasale AL and Cohen M: Garlic for the common cold. Cochrane Database Syst Rev 3: CD006206, 2012.
8. Lee IC, Kim SH, Baek HS, *et al*: The involvement of Nrf2 in the protective effects of diallyl disulfide on carbon tetrachloride-induced hepatic oxidative damage and inflammatory response in rats. Food Chem Toxicol 63: 174-185, 2014.
9. Truong D, Hindmarsh W and O'Brien PJ: The molecular mechanisms of diallyl disulfide and diallyl sulfide induced hepatocyte cytotoxicity. Chem Biol Interact 180: 79-88, 2009.
10. Arunkumar R, Sharmila G, Elumalai P, *et al*: Effect of diallyl disulfide on insulin-like growth factor signaling molecules involved in cell survival and proliferation of human prostate cancer cells in vitro and in silico approach through docking analysis. Phytomedicine 19: 912-923, 2012.
11. Song JD, Lee SK, Kim KM, *et al*: Molecular mechanism of diallyl disulfide in cell cycle arrest and apoptosis in HCT-116 colon cancer cells. J Biochem Mol Toxicol 23: 71-79, 2009.
12. Nkrumah-Elie YM, Reuben JS, Hudson AM, *et al*: The attenuation of early benzo (a) pyrene- induced carcinogenic insults by diallyl disulfide (DADS) in MCF-10A cells. Nutr Cancer 64: 1112-1121, 2012.
13. Ling H, Wen L, Ji XX, *et al*: Growth inhibitory effect and Chk1-dependent signaling involved in G2/M arrest on human gastric cancer cells induced by diallyl disulfide. Braz J Med Biol Res 43: 271-278, 2010.
14. Jun Z, Suzuki M, Xiao J, Wen J, Talbot SG, Li GC and Xu M: Comparative effects of natural and synthetic diallyl disulfide on apoptosis of human breast-cancer MCF-7 cells. Biotechnol Appl Biochem 52: 113-119, 2009.
15. Zhang XH, Zou ZQ, Xu CW, Shen YZ and Li D: Myricetin induces G2/M phase arrest in HepG2 cells by inhibiting the activity of the cyclin B/cdc2 complex. Mol Med Rep 4: 273-277, 2011.
16. Sankari SL, Masthan KM, Babu NA, Bhattacharjee T, Elumalai M: Apoptosis in cancer - an update. Asian Pac J Cancer Prev 13: 4873-4878, 2012.
17. Czepukojc B, Baltes AK, Cerella C, *et al*: Synthetic polysulfane derivatives induce cell cycle arrest and apoptotic cell death in human hematopoietic cancer cells. Food Chem Toxicol 64: 249-257, 2014.
18. Tang H, Kong Y, Guo J, *et al*: Diallyl disulfide suppresses proliferation and induces apoptosis in human gastric cancer through Wnt-1 signaling pathway by upregulation of miR-200b and miR-22. Cancer Lett 340: 72-81, 2013.
19. Haneji T, Hirashima K, Teramachi J and Morimoto H: Okadaic acid activates the PKR pathway and induces apoptosis through PKR stimulation in MG63 osteoblast-like cells. Int J Oncol 42: 1904-1910, 2013.
20. Hui C, Jun W, Ya LN and Ming X: Effect of *Allium sativum* (garlic) diallyl disulfide (DADS) on human non-small cell lung carcinoma H1299 cells. Trop Biomed 25: 37-45, 2008.
21. Tan H, Ling H, He J, Yi L, Zhou J, Lin M and Su Q: Inhibition of ERK and activation of p38 are involved in diallyl disulfide induced apoptosis of leukemia HL-60 cells. Arch Pharm Res 31: 786-793, 2008.
22. Altonsy MO, Habib TN and Andrews SC: Diallyl disulfide-induced apoptosis in a breast-cancer cell line (MCF-7) may be caused by inhibition of histone deacetylation. Nutr Cancer 64: 1251-1260, 2012.
23. Duong HQ, Hwang JS, Kim HJ, Seong YS and Bae I: BML-275, an AMPK inhibitor, induces DNA damage, G2/M arrest and apoptosis in human pancreatic cancer cells. Int J Oncol 41: 2227-2236, 2012.
24. Paul P, Rajendran SK, Peuhu E, Alshatwi AA, Akbarsha MA, Hietanen S and Eriksson JE: Novel action modality of the diterpenoid anisomelic acid causes depletion of E6 and E7 viral oncoproteins in HPV-transformed cervical carcinoma cells. Biochem Pharmacol 89: 171-184, 2014.
25. Zhang Z, Wang CZ, Du GJ, *et al*: Genistein induces G2/M cell cycle arrest and apoptosis via ATM/p53-dependent pathway in human colon cancer cells. Int J Oncol 43: 289-296, 2013.
26. Li B, Zhao J, Wang CZ, Searle J, He TC, Yuan CS, Du W: Ginsenoside Rh2 induces apoptosis and paraptosis-like cell death in colorectal cancer cells through activation of p53. Cancer Lett 301: 185-192, 2011.
27. Ding L, Huang Y, Du Q, *et al*: TGEV nucleocapsid protein induces cell cycle arrest and apoptosis through activation of p53 signaling. Biochem Biophys Res Commun 445: 497-503, 2014.
28. Takahashi H, Chen MC, Pham H, *et al*: Baicalein, a component of *Scutellaria baicalensis*, induces apoptosis by Mcl-1 down-regulation in human pancreatic cancer cells. Biochim Biophys Acta 1813: 1465-1474, 2011.
29. Lv C, Sun W, Sun H, Wei S, Chen R, Wang B and Huang C: Asperolide A, a marine-derived tetranorditerpenoid, induces G2/M arrest in human NCI-H460 lung carcinoma cells, is mediated by p53-p21 stabilization and modulated by Ras/Raf/MEK/ERK signaling pathway. Mar Drugs 11: 316-331, 2013.